Performance analysis of a medium-sized industrial reverse osmosis brackish water desalination plant

M. A. Al-Obaidi [1,2], A. A. Alsarayreh [1], A. M. Al-Hroub [3], S. Alsadaie [4], and I. M. Mujtaba [1,*]

[1] School of Engineering, Faculty of Engineering and Informatics. University of Bradford. Bradford, West Yorkshire BD7 1DP, UK
[2] Middle Technical University, Iraq – Baghdad
[3] Senior Chemical Engineer, Energy and Water Directorate, Arab Potash Company, Jordan
[4] Chemical Engineering Department, Faculty of Engineering, University of Sirte, Sirte, Libya
*Corresponding author, Tel.: +44 0 1274 233645
E-mail address: I.M.Mujtaba@bradford.ac.uk

Abstract

The implementation of Reverse Osmosis (RO) technology is noticeably increased to produce freshwater from brackish and seawater resources. In this work, performance analysis of a multistage multi pass medium-sized spiral wound brackish water RO (BWRO) desalination plant (1200 m³/day) of Arab Potash Company (APC) located in Jordan is evaluated using modelling and simulation. For this purpose, a mathematical model for the spiral wound RO process based on the principles of solution diffusion model is developed. The model is then used to simulate the operating conditions of low-salinity brackish water RO (BWRO) desalination plant. The results obtained are then compared against the real industrial data of BWRO desalination plant of APC which shows a high-level of consistency. Finally, the model is used to analysis the impact of the operating parameters such as salinity, pressure, temperature, and flow rate on the plant performance. The sensitivity analysis confirms that both feed flow rate and operating pressure as the critical parameters that positively affect the product salinity.

Keywords: Reverse Osmosis; Spiral wound Module; Brackish Water Desalination, Modelling; Simulation, Performance Analysis

1. Introduction

The Red Sea and groundwater are considered as the most important available resources of water in Jordan which spread over 80% of the country in different quantity and quality [1]. Desalination of seawater and brackish water is an important choice to provide potable, agricultural and reuse water especially in the regions suffering from water scarcity [2-4]. Interestingly, brackish water desalination plants

1

are considerably used in Jordan as a potential source of freshwater specially to cope water scarcity and to rectify the shortage of a good quality water in Jordan [5].

The Reverse Osmosis (RO) technology has been increasingly considered as one of the cheapest and promising methods for salinity reduction [6-9]. Having said this, the RO technology is a successful process to remove almost all constitutes of dissolved solids in sea and brackish water. The membrane modules are provided in several types including hollow fiber, plate and frame, tubular and spiral wound. However, spiral wound module is the most popular among RO membrane modules [10]. The RO and especially spiral wound module is mainly designed with several stages and orders to consider the quality of the produced water and economics. Interestingly, this technology has witnessed a rigorous development especially in improving both the water quality and recovery. This has happened due to the development of a new generation of RO membranes that commensurate with high-level of salt rejection and water permeation at a realistic energy consumption. Moreover, this technology is more flexible to be scaled up (ranging from small-sized to large-sized) and requires lower operating cost and energy consumption compared to thermal processes like multistage flash distillation (MSF) [8,11,12]. Therefore, there are much interest to model and optimize the RO process to satisfy specific requirements of water.

A thorough review of the open literature confirms several attempts of spiral wound RO modelling based on the principles of solution diffusion model and irreversible thermodynamic model [13-17]. The models developed are used to quantify the transport phenomenon of water and solute through the membrane.

In this respect, the area of seawater and brackish water RO desalination plant modelling of different sizes with various limitations and assumptions has been carried out by several studies based on spiral wound module. This in turn provides several faces of semi-empirical models that predict the plant performance with the aid of experimental data. Several examples of the models developed for this purpose and based on solution diffusion model are illustrated in the next.

Abbas and Al-Bastaki [11] and Abbas [14] presented a semi-rigorous model to investigate the performance of a small-sized BWRO desalination plant of four pressure vessels arranged in three tapered stages. Each pressure vessel holds three spiral wound membranes of Dow/FilmTec BW30-400 membranes in series. Geraldes et al. [18] developed a numerical model for spiral wound two stage seawater RO desalination plant (1000 m³/day) and used for simulation and optimisation. Majali et

al. [19] analysed the performance of the Sharjah BW small-sized RO plant (production capacity of 237.5 m³/day) using a rather simple model. The plant contains two stages of 30 and 12 pressure vessels, respectively, each pressure vessel holding six membranes connected in series. Lee et al. [10] studied the dynamic characteristics and process operation of the Jeddah large-sized RO desalination plant operated in the Kingdom of Saudi Arabia (production capacity of 56800 m³/day). For this purpose, a dynamic model is developed based on the work of Oh et al. [15], Marriott and Sørensen [20], Lee and Lueptow [21]. Kaghazchi et al. [16] developed a steady state model to analyse the performance of two industrial seawater RO plants (capacity of 3456 m³/day and 52 m³/day respectively) based on FilmTec SW30HR-380 spiral wound membrane modules. The first seawater RO plant contains 294 parallel pressure vessels while the second RO plant contains 32 pressure vessels connected in series. Each pressure vessels holds 7 membranes in series. Ruiz-Saavedra et al. [22] presented a simple design method that comprises a sophisticated modelling and originally conceived for the application to subterranean BWRO desalination plants in the Canary Islands, Spain. The input data of chemical composition, pH, SDI, temperature, plant production and membrane manufacturer design guideline are required to design the RO system and operating pressure that ensures the product quality.

However, most studies are carried out for small-sized plants and few studies have been conducted for medium and large-sized BWRO desalination plants. Also, the impact of operating temperature on transport parameters has not been considered. Also, the majority of these models are developed under the assumptions of constant physical properties and mass transfer coefficient.

This research is mainly related to the BWRO desalination plant of APC producing low-salinity water. To the best of the authors' knowledge, there has not yet been any study to model the medium-sized BWRO plant and to analyse the plant performance under various operational parameters. Therefore, the primary aim of this study is to develop a steady state numerical model of algebraic and non-linear equations for spiral wound RO process based on the principles of solution diffusion model. Then, a full model of multi-stage multi-pass BWRO of APC is developed to simulate the actual plant. The characteristics of the model developed in this paper are as follows:

- the variation of model transport parameters is considered against the variation of feed temperature and fouling factor;
- the osmotic pressure in both feed and permeate channels is investigated using the empirical correlation of Toray membrane USA Inc. (membrane manufacturer);
- new solute rejection and recovery rate correlations are derived from the material balance equations.

Due to the existence of real data gathered from the plant operator, the model developed will be examined and validated against reliable experimental data. Then, the plant performance will be explored against the operating conditions via a sensitivity analysis study.

Note that the model developed has the capacity to select the number of stages, pressure vessels, membrane numbers, and stream connections to simulate any size of RO plant. Therefore, it is a ready tool that can be used to simulate, analyse and optimise the performance of any size of RO plant.

2. BWRO desalination plant of APC

The Arab Potash Company (APC) is the eighth largest potash producer worldwide. APC was commercially operated on 1956 in the Hashemite Kingdom of Jordan as an Arab commercial enterprise and has a 100-year concession for the future (1956-2058) from the Jordanian government, which grants it exclusive rights to manufacture and market minerals extracted from the Dead Sea. The annual production of APC reaches 2.0 million tons of potash, as well as bromine and sodium chloride [23]. The BWRO desalination plant of APC (supplier: EnviroMatch, Inc.) with a nominal capacity of 1200 m³/day is included in the power plant to produce pure water with low-salinity where it is totally demineralized (i.e. conductivity will be less than 1 μs) after delivering to Ion Exchangers. The feed water of the desalination plant (pH = 7.45-7.59) is fed from groundwater salt wells and pumped into collection tanks at APC, where it is then pumped directly to the water treatment plant. Table 1 shows the composition analysis of the feed water. Specifically, there is no treatment at this stage because the wells water is considered suitable as a feed due to low salinity of feed water of about 1100 ppm [24].

Table 1. Feed water composition analysis

Conductivity μs/cm	pH	TDS (ppm)	Turbidity (NTU)	Alkalinity (HCO_3^-) (ppm)	SiO_2 (ppm)	Na^+ (ppm)	Total hardness (ppm)	Cl^- (ppm)
1983.06	7.59	1098.62	1	61	23.6	144.71	1367.17	346.26

The desalination plant constitutes of several separate operations including; pre-treatment, high-pressure pumps, RO membrane module, permeate water re-mineralization treatment (post treatment), and brine disposal. The pre-treatment of BWRO desalination plant is an important to increase the efficiency and lifetime of the membranes. The pre-treatment unit of RO plant is the media-filter stage which contains three multi-media filters consisting of anthracite, silica, and garnet to remove suspended and colloidal particles by media filtration while the water flows through a bed of filter media. Then, scale inhibitor is used to control carbonate scaling, sulphate scaling and calcium fluoride scaling on membranes. The chemical used is from NALCO Company (Permatreat 191T). The last unit of pre-treatment stage is the filtration system composes three cartridge filters, each one come complete with (12) 2.5" x 40" (1 micron) cartridges. It acts like a safety device that protects the membranes and the high-pressure pumps.

The second unit of BWRO plant consists of two high-pressure pumps and one stand-by pump at both 1st and 2nd passes, respectively of RO plant to drive the feed water into the membranes. The pumps (type: Goulds pumps, ITT) are multistage vertical centrifugal with wetted parts constructed from 316 SS material and Motor Efficiency 91.7%.
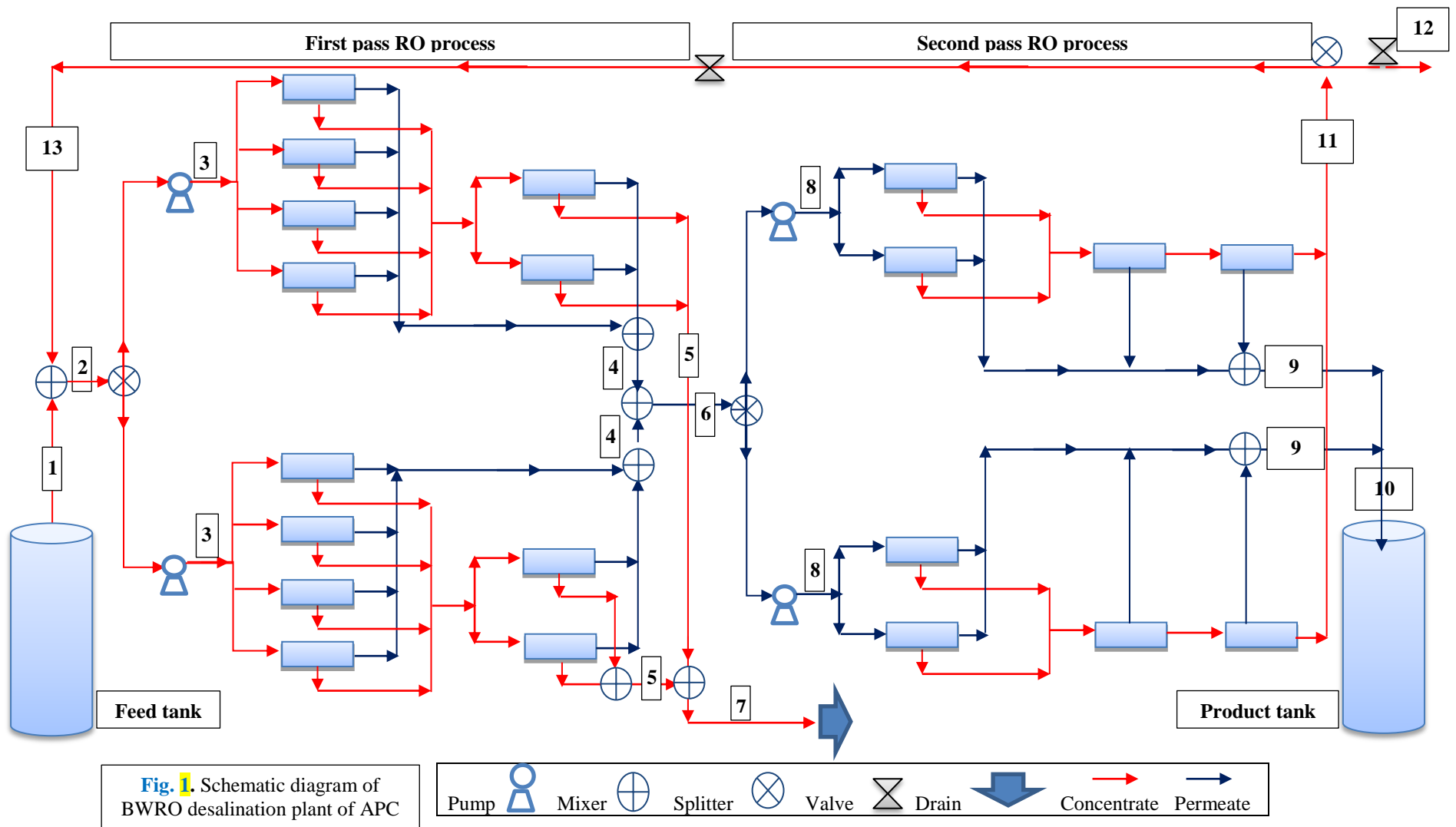
The third unit of BWRO desalination plant is the RO modules. Fig. 1 shows the BWRO plant flowsheet which contains 20 pressure vessels and 120 membranes. The configuration of BWRO plant comprises both retentate and permeate reprocessing. The 1st pass contains two parallel stages of six pressure vessels with arrangement (4:2) while the 2st pass contains four pressure vessels with arrangement (2:1:1). Specifically, each pressure vessels holds 6 nominally identical spiral wound membranes type TMG20D-400 (Toray Membrane USA Inc.) connected in series with 37.2 m² as an effective area. This in turn is set to increase the recovery rate of each pressure vessel. Sodium Hydroxide (NaOH) (salinity 32% Wt.) is dosed on the

permeate product of the 1st pass (feed stream of the 2nd pass) to control the pH to 8.5, the purpose to increase the pH is to convert CO_2 to HCO_3^-, which can be rejected in the 2nd pass, thus reducing the load on the mixed bed downstream. In other words, the mixed bed composes of both strong cation resin and strong anion resin, in which the latter can remove most of the negatively charged ions (as HCO_3^-), and when this ion is removed in the 2nd RO pass, it will reduce the load on the mixed bed, thus it can handle more concentrations before it requires regeneration. It is also important to mention that removing the CO_2 by adding NaOH is the method used in this RO system, otherwise, a "degasifier" unit is needed. The total permeate of the 1st pass is collected in a separate permeate storage tank (at atmospheric pressure) and is pumped as the feed stream of the 2nd pass. Therefore, two forwarding pumps are used at the 2nd pass to drive water through the membranes of 2st pass (Fig. 1). The permeate streams of all the pressure vessels of the 2st pass are blended to form the product stream of the plant that collected in a separate product tank. The product salinity is around 2 ppm at a relatively daily production capacity of 1200 m³/day. This low-salinity product water of 2nd pass is pumped using a high-pressure pump and delivered into polishing unit while the high salinity retentate stream of the 1st pass is disposed off into a drainage system that collects water from cooling tower drainage and neutralized water resulted from resin regeneration. pH is controlled and monitored to be neutralized before discharging to drain system. This final water is called "reclaiming water" that is used as in one of three production plants of APC called as Hot Leach Plant[1] (HLP). However, the low salinity retentate of the 2nd pass is recycled back to be coupled with the main stream of feed water. This in turn forms the main stream of the 1st pass that pressurised using high-pressure pumps.

The mixed bed polisher which constitutes the last stage of BWRO desalination plant is used to remove all impurities through ion exchange as water passes over separate layers of resin. The first layer contains a cation resin to remove positively charges particles while the second layer contains an anion resin to remove negatively charged particles. Then, the high-purity water is collected in a make-up tank and pressurised into boilers using high-pressure pumps.

---

[1] HLP plant uses the combined brine water of the Dead Sea, brackish water, and several processes sewage water of the power plant and retentate of first pass RO plant. This water is used to make the final product of KCL.

1

2

3

Fig. 1. Schematic diagram of BWRO desalination plant of APC

First pass RO process

Second pass RO process

Feed tank

Product tank

Pump   Mixer   Splitter   Valve   Drain   Concentrate   Permeate

3. The APC Process Model

The following assumptions were made to develop the process model:

- Steady state operation.
- The solution diffusion model of Lonsdale et al. [25] is used to elucidate the transport phenomenon of water and solute.
- The membrane is characterised as a porous flat sheet with spacers.
- The membrane characteristics and the channel geometries are assumed constant.
- The film theory model is used to quantify the concentration polarization.
- Negligible pressure drop in the freshwater side due to very low permeate velocity and a constant pressure of 1 atm is assumed.
- Isothermal process means constant temperature at the feed and permeate channels.
- The pressure drop in the feed channel per each element is calculated using the correlation of Da Costa et al. [26] where the spacer characteristics are applied to characterize the pressure drop.

The solution diffusion model is used to elucidate the transport phenomenon of permeate and solute through the membrane. The total water flux Q_p (m³/s) is given in Eq. (1)

$$Q_p = A_{w(T)} \, NDP_{fb} \, A_m$$

(1)

$A_{w(T)}, NDP_{fb}, A_m$ (m/s atm, atm, m²) are water permeability constant at operating temperature, calculated by Eq. (2), net driving pressure of feed and brine, and membrane area, respectively. Operating temperature mainly affects the RO process. Therefore, the temperature correction factor will be considered in Eq. (2) based on the reference value at 25 °C to estimate the actual water transport parameter

$$A_{w(T)} = A_{w(25\,C)} \, TCF_p \, F_f \qquad (2)$$

$A_{w(25\,C)}, TCF_p, F_f$ (m/s atm, dimensionless) are the water permeability constant at 25 °C, the temperature correction factor of permeate which is calculated based on the operating and reference temperature (25 C°) and the fouling factor, respectively. The

following equations are used to estimate the temperature correction factor at standard conditions and proposed by Toray Membrane USA Inc. (membrane manufacturer, [27])

$$TCF_p = \exp[0.0343\,(T - 25)] \qquad < 25\,°C$$

(3)

$$TCF_p = \exp[0.0307\,(T - 25)] \qquad > 25\,°C$$

(4)

The driving pressure of feed and brine is estimated using Eq. (5)

$$NDP_{fb} = P_{fb} - P_p - \pi_b + \pi_p$$

(5)

$P_{fb}, P_p, \pi_b, \pi_p$ and T (atm, °C) are feed brine pressure, permeate pressure, osmotic pressure of bulk brine and permeate and operating temperature, respectively. The feed brine pressure P_{fb} (atm) decreases along the feed side due to the pressure drop caused by friction. Therefore, it is calculated in the counter of Eq. (6)

$$P_{fb} = P_f - \frac{\Delta P_{drop,E}}{2}$$

(6)

P_f and $\Delta P_{drop,E}$ (atm) are the operating feed pressure and the pressure drop along the membrane element, respectively. $\Delta P_{drop,E}$ (atm) represents the difference between the feed P_f (atm) and retentate pressures P_r (atm) as given in Eq. (7) [26]. This equation illustrates the impact of feed spacer on the pressure drop that separates the surfaces of adjacent membrane envelopes and promotes the turbulence and mass transfer coefficient at the feed channel.

$$\Delta P_{drop,E} = \frac{9.8692 x 10^{-6}\, A^*\, \rho_b\, U_b{}^2\, L}{2 d_h\, Re_b^n}$$

(7)

A^*, $n, \rho_b, U_b,\ L, d_h$ and Re_b (dimensionless, kg/m³, m/s, m, dimensionless and dimensionless) are the feed spacer characteristic, bulk density, bulk velocity, membrane length, hydraulic diameter of the feed spacer channel, and Reynolds

number, respectively. The parameter ($\frac{A^*}{Re^n}$) represents the total drag force, which is function of Reynolds number and spacer characteristic. The Reynolds number and bulk velocity are calculated as

$$Re_b = \frac{\rho_b\, d_h\, Q_b}{t_f\, W\, \mu_b}$$

(8)

$$U_b = \frac{Q_b}{W\, t_f\, \epsilon}$$

(9)

Q_b, W, t_f and ϵ (m³/s, m, m and dimensionless) are the bulk flow rate (calculated as the average value of feed Q_b (m³/s) and retentate flow rates Q_r (m³/s) as described in Eq. (10), membrane width, feed channel height and void fraction of the feed spacer, respectively. Da Costa et al. [26] tested the pressure drop caused by seven different types of feed spacers stuffed in the membrane feed channel type Koch Systems, HFK-131. This test provides the characteristics of each feed spacer including A^* and n of each feed spacer. This accelerates the calculation of pressure drop per each feed spacer type using the proposed Eq. (7)

$$Q_b = \frac{Q_f + Q_r}{2} \qquad (10)$$

The bulk and permeate osmotic pressures are calculated using the empirical equation proposed by Toray Membrane USA Inc. (membrane manufacturer) [27]

$$\pi_b = 0.7994\, C_b\, [1 + 0.003\, (T - 25)]$$

(11)

$$\pi_p = 0.7994\, C_p\, [1 + 0.003\, (T - 25)]$$

(12)

C_b and C_p (kg/m³) are the bulk and permeate salinities, respectively. The bulk salinity C_b (kg/m³) is taken as the average of feed and retentate salinities as can be shown in Eq. (13)

$$C_b = \frac{C_f + C_r}{2}$$

(13)

The solute flux through the membrane Q_s (kg/m² s) is calculate by Eq. (14)

$$Q_s = B_{s(T)}\left(C_w - C_p\right)$$

(14)

$B_{s(T)}, C_w$ (m/s, kg/m³) are the solute transport parameter at operating temperature, calculated in Eq. (15), solute salinity at the membrane wall, respectively. The impact of operating temperature on solute transport parameter is calculated based on the reference value at 25 °C

$$B_{s(T)} = B_{s(25\,C)}\, TCF_s$$

(15)

$B_{s(25\,C)}$ (m/s) is the solute transport parameter at 25 °C. The temperature correction factor of solute TCF_s (dimensionless) at standard conditions is calculated based on the operating temperature and based on the proposed correlation used by the supplied by membrane manufacturer (Toray)

$$TCF_s = 1 + 0.05\,(T - 25) \qquad\qquad\qquad < 25\,°C$$

(16)

$$TCF_s = 1 + 0.08\,(T - 25) \qquad\qquad\qquad > 25\,°C$$

(17)

It is assumed that the analytical film theory is valid to count the concentration polarization as a function of mass transfer coefficient k (m/s) [28]. This means that the concentration C_w (kg/m³) at the membrane surface is slightly bigger than the bulk concentration C_b (kg/m³) due to diffusion from the bulk flow.

$$C_w = C_p + \left(\frac{C_f + C_r}{2} - C_p\right) exp\left(\frac{Q_p/A_m}{k}\right)$$

(18)

The mass transfer coefficient equation of Da Costa et al. [26] is used which comprises the Reynolds number Re (-), Schmidt number Sc (-), diffusivity parameter D_b (m²/s) and feed characteristics. The physical properties are predicted using the model water equations of Koroneos [29].

$$k = 0.664 \, k_{dc} \, Re_b^{0.5} \, Sc^{0.33} \left(\frac{D_b}{d_h}\right)\left(\frac{2d_h}{L_f}\right)^{0.5}$$

(19)

$$Sc = \frac{\mu_b}{\rho_b \, D_b}$$

(20)

$$\rho_b = 498.4 \, m_f + \sqrt{\left[248400 \, m_f^2 + 752.4 \, m_f \, C_b\right]}$$

(21)

$$m_f = 1.0069 - 2.757 x 10^{-4} \, T$$

(22)

$$D_b = 6.725 10^{-6} \, exp\left\{0.1546 10^{-3} \, C_b - \frac{2513}{T+273.15}\right\}$$

(23)

$$\mu_b = 1.234 x 10^{-6} \, exp\left\{0.0212 \, C_b + \frac{1965}{T+273.15}\right\}$$

(24)

k_{dc}, d_h, L_f, ρ_b and μ_b (dimensionless, m, m, kg/m³ and kg/m s) are constant in Eq. (19), which is related to the feed spacer characteristics, hydraulic diameter of the feed spacer channel, length of filament in the spacer mesh, bulk density, and kinematic viscosity, respectively.

The total mass and solute balance of the whole unit gives

$$Q_f = Q_r + Q_p \tag{25}$$

$$Q_f \, C_f - Q_r \, C_r = Q_p \, C_p \tag{26}$$

Based on Eqs. (25) and (26), a new correlation for the total recovery Rec (dimensionless) is developed as follows:

$$Q_f \, C_f - Q_r \, C_r - Q_p C_r = Q_p \, C_p - Q_p C_r \tag{27}$$

$$Q_f \, C_f - C_r(Q_r + Q_p) = Q_p \, C_p - Q_p C_r \tag{28}$$

$$Q_f \, (C_f - C_r) = Q_p(C_p - C_r) \tag{29}$$

$$Rec = \frac{Q_p}{Q_f} = \frac{(C_r - C_f)}{(C_r - C_p)} \tag{30}$$

Moreover, the solute flux can be estimated following this

$$Q_s = \frac{Q_p\, C_p}{A_m}$$

(31)

Substituting Eq. (31) in Eq. (14) yields

$$B_{s(T)}\left(C_w - C_p\right) = \frac{Q_p\, C_p}{A_m}$$

(32)

Dividing Eq. (32) by C_f yields

$$\frac{B_{s(T)}(C_w - C_p)}{C_f} = \frac{Q_p\, C_p}{A_m\, C_f}$$

(33)

Simplify Eq. (33) gives

$$Rej_{real} = \frac{Q_p\,(1 - Rej)}{A_m\, B_{s(T)}}$$

(34)

Rej_{real} and Rej (dimensionless) are the real solute rejection and observed rejection as given in Eqs. (35) and (36)

$$Rej_{real} = \frac{C_w - C_p}{C_w}$$

(35)

$$Rej = \frac{C_f - C_p}{C_f}$$

(36)

Re-arrangement of Eq. (34) gives a new correlation for the accurate water flux J_w (m/s)

$$J_w = \frac{B_{s(T)}\, Rej_{real}}{(1 - Rej)}$$

(37)

Assuming Rej equals Rej_{real} yield a new correlation for solute rejection can be estimated as

$$Rej = \left(1 + \frac{B_{s(T)}}{J_w}\right)^{-1}$$

(38)

The average permeate salinity at the permeate channel and retentate salinity are estimated using the proposed correlations of Lawrence [30].

$$C_p = \frac{C_f}{Rec}\left[1 - (1 - Rec)\right]^{(1-Rej)}$$

(39)

$$C_r = C_f\left[1 - Rec\right]^{-Rej} \tag{40}$$

The model equations presented above is coded and solved within gPROMS software suite.

The feasible steady state model developed above for an individual spiral wound RO process will be used to build and characterise the complete mathematical modelling of BWRO plant of APC that defines the stream connections and plant performance. The complete mathematical model is given in Table A.1 in Appendix A. The model prediction is compared against the actual plant data and used then to analyse the plant performance under a varied set of operating parameters.

4. Model validation with APC data

Table 2 shows the details of feed water fed to the BWRO plant, design specifications and plant operating conditions while more detail descriptions of membrane and element specifications, spacer type, and the water and salt permeability constants are given in Table 3. Note that the feed spacer specification including A, n, ε and k_{dc} are collected from Abbas [14] and given in Table 3.

The RO plant is working under low pressure conditions due to the use of low salinity feed water. This pressure is considered to overcome the osmotic pressure, friction losses and the membrane resistance. However, the applied design has resulted in an average low salinity product of 1.96 ppm. The operating parameters of the 1st pass and 2nd pass of BWRO plant including feed flow rate, salinity, pressure, temperature, recovery and salt rejection, product salinity, and retentate were taken periodically

15

twice every day. Note that Table 4 shows the minimum and maximum values of operating parameters for the period between 15/2/2018 to 15/3/2018. However, the average value of any operating parameters is considered as an actual operating data. The maximum concentration polarisation is occurred in the 1st pass of RO plant. Therefore, the expectation that fouling propensity (scaling fouling) is higher at the beginning membranes of each pressure vessel [31]. However, the conceptual designs of multi-stage RO process of APC company which characterised by the use of two parallel pressure vessels in the second stage of the 1st pass would increase the operating flow rate at this stage that aids to reduce the propensity of fouling. Also, it should be noted that the data were collected from the plant after renewing the membranes of the 1st pass. Therefore, the fouling situation has been controlled and its impact on plant performance is ignored albeit for this stage. Consequently, the fouling factor (F_f) in Eq. (2) is assumed to be 1.

The comprehensive model for the multi-stage multi-pass BWRO plant of APC is built up and solved in gPROMS software. The design parameters shown in Table 3 are used to solve the model developed and then used in the subsequent simulations. For a given operating conditions of feed salinity, flow rate, pressure, and temperature, the proposed model is able to predict the operating parameters at any position of the plant including the total rejection and recovery rate. Table 4 shows comparison between the plant data of BWRO plant and model prediction at several positions along the 1st and 2nd passes of the plant. Table 4 shows that both actual operating results and corresponding model predictions were consistent (absolute error is around 6%). It is noteworthy to mention that the BWRO plant of APC produces low-salinity water of average salinity 1.96 ppm. This in turn reflects the advantage of implementing the 2nd pass as a pre-treatment step of the produced permeate of the 1st pass. Undoubtedly, this would reduce the extent of concentration polarisation and enhance the mass transfer coefficient. Moreover, the use of low salinity water as the feed stream of 2nd pass, there is no fear of fouling or scaling issues on the membrane surface. Also, it is important to mention that the design of the two-pass system of BWRO plant of APC is characterised by collecting the permeate of the 1st to be the feed stream of the 2nd pass. Therefore, the retentate stream of 2nd pass would be in a lower concentration than the feed concentration of the plant.

Table 2. Design specification for an industrial BWRO plant of APC [24]

Operation condition		
Parameter	Unit	Value
Feed water salinity	ppm	1098
pH of feed water	-	7.45 -7.55
Feed water flow rate	m³/h	74
Feed temperature	°C	25
Feed pressure to the 1st pass	atm	9.220
Feed pressure to the 2st pass	atm	9.832
Daily production capacity	m³/day	1200
Average product salinity	ppm	1.96
Total system rejection	%	99.80

Table 3. Specifications of the spiral wound membrane element and transport parameters

Parameter	Value
Membrane supplier	Toray Membrane USA Inc.
Membrane type and configuration	TMG20D-400, Ultra low pressure BWRO, spiral wound, polyamide thin-film Composite
Feed and permeate spacer thickness t_f, t_p (m)	8.6×10^{-4} (34 mils), 5.5×10^{-4}
Hydraulic diameter of the feed spacer channel d_h (m)	8.126×10^{-4}
Effective membrane area A (m²)	37.2
Membrane length L and width W (m)	1 and 37.2
Maximum operating pressure (atm)	40.464
Maximum pressure drop per element (atm)	0.986923
Maximum operating temperature (°C)	45
Minimum salt rejection (%)	99.5
$A_{w\,(T_o)}$ (m/ atm s) at 25 °C	9.6203×10^{-7}
$B_{s(T_o)}$ (NDMA) (m/s) at 25 °C	1.61277×10^{-7}
Spacer type	NALTEX-129
length of filament in the spacer mesh L_f (m)	2.77×10^{-3} *
$A^{'}$ (dimensionless)	7.38
n (dimensionless)	0.34
ε (dimensionless)	0.9058
k_{dc} (-)	1.501

Table 4. Comparison of the actual Arab Potash RO plant and model predictions 2

1st pass RO process							
Parameter	Position	Experimental results				Model	Error %
		Unit	Min.	Max.	Average		
Feed water salinity	1	ppm	1098.62	1098.62	1098.62	--	--
Feed flow rate	1	m³/h	74	74	74	--	--
Plant feed flow rate	2	m³/h	84	84	84	--	--
Plant feed salinity	2	ppm	997	997	997	--	--
Temperature	2	°C	25	25	25	--	--
Pressure	3	atm	9.118	9.322	9.220	--	--
Feed flow rate	3	m³/h	42	42	42	--	--
Salinity	3	ppm	997	997	997	--	--
Permeate flow rate	4	m³/h	29.1	29.6	29.233	29.423	-0.65
Retentate pressure	5	atm	8.2335	8.5737	8.3809	8.4420	-0.72
Retentate flow rate	5	m³/h	12.5	12.6	12.57	12.576	-0.05
Feed flow rate	6	m³/h	58.2	59.2	58.466	58.847	-0.65
Rejection	6	(-)	95.4	95.7	95.466	95.460	0.00
Recovery rate	6	(-)	70	70.2	70.08	70.056	0.03
Retentate flow rate	7	m³/h	25	25.2	25.14	25.152	-0.05
2nd pass RO process							
Pressure	8	atm	9.730	9.866	9.832	--	--
Permeate salinity	9	ppm	1.5234	3.0469	1.96	2.0358	-3.86
Permeate flow rate	9	m³/h	24.9	25.1	24.57	24.131	1.78
Rejection	9	(-)	92	95.5	95.5	95.501	-1.59
Recovery rate	9	(-)	84.1	84.9	83.5	82.012	1.78
Permeate salinity	10	ppm	1.5234	3.0469	1.96	2.0358	-3.86
Permeate flow rate	10	m³/h	49.8	50.2	49.14	48.262	1.78
Retentate flow rate	11	m³/h	10	10	10	10.584	-5.84
Retentate salinity	11	ppm	245	245	246	242.31	1.49
Recycled salinity	13	ppm	245	245	245	242.31	1.09
Recycled flow rate	13	m³/h	10	10	10	10.584	-5.84

3

5. Performance analysis of APC: Impact of operating parameters 4

It is important to analyse the plant performance against the variation of operating 5
conditions which aids to improve the product quality and process optimisation. The 6
model presented in Section 3 and Table A.1 in Appendix A is used to carry out a 7
simulation study of BWRO plant of APC. The selected indicators of the plant 8
performance are including the total plant solute rejection, 1st pass and 2nd pass 9
rejections, plant recovery, 1st pass and 2nd pass recoveries, product salinity and plant 10
retentate salinity. However, the investigated operating conditions are including feed 11
water feed salinity, feed water feed flow rate, operating pressure, and temperature. 12
The simulation results and plant data shown in Table 4 were considered as the base 13

case before carrying out the sensitivity analysis. It is decided to investigate the impact of a 20% variation of operating conditions against the plant performance. However, the considered variation of temperature is corresponding to the season variation (summer and winter) in the region of Dead Sea.

5.1 Impact of feed salinity

Undoubtedly, the quality of any brackish water system is generally deteriorated with time. Therefore, it is important to investigate this concern albeit at a small increase of feed water salinity. Model simulations are conducted to investigate the impact of a 20% increase of feed water salinity on the plant performance from the basic value of 1098.62 ppm to 1318.34 ppm at a step change of 1%. This simulation is carried out at fixed operating plant pressure 9.22 atm, water feed flow rate 74 m³/h and temperature 25 °C. Therefore, it is assumed that the plant is initially running at initial feed water salinity of 1098.62 ppm and recycle stream conditions (position 13 in Table 4) and 1% increase of feed water salinity is occurred. However, the forward simulation is carried out at 2% increase of feed water salinity while the other operating parameters are set to the initial case and so on. For this simulation, the inlet plant feed salinity (position 2 in Fig. 1) is calculated using Eq. (2) in Table A.1 in Appendix A by considering fixed feed water flow rate, recycle salinity and recycle flow rate as calculated within the initial run. Most importantly, due to mixing process of feed water and recycled streams at the point 2 of Fig. 1, the extent of the inlet feed flow rate and salinity are changed dynamically for a period of time until getting to steady state conditions. Therefore, the criteria of solving this concern was to run the developed model in an iteration loop to get constant conditions of plant feed stream. At this point, the results of model simulation are considered for performance analysis. It is observed that 20% increase of feed water salinity has inconsiderable impact on total plant rejection (99.798% - 99.760%), 1st pass rejection (95.503% - 95.263%), 2nd pass rejection (95.521% - 94.940%). The low considered variation may interpret the slight reduction of solute rejection. Therefore, increasing the feed water salinity causes a significant increase of product and plant retentate salinity as can be seen in Fig. (2). Statistically, the product salinity increases from 1.99 ppm to 2.98 ppm, while a significant increase from 243.8 ppm to 456.0 ppm is occurred in retentate salinity as a result of increasing feed water salinity (Fig. 2). As the feed salinity increases, the membrane surface concentration and osmotic pressure would increase which retards

product flux through the membrane. This in turn elevates the product and plant 1

retentate salinity. In this respect, it is fair to expect that increasing the feed salinity 2

would increase the bulk concentration of all the membrane modules, which already 3

causes a reduction of mass transfer coefficient especially at the membranes located in 4

the 1st pass of the plant. This is readily plotted in Fig. 3 where it shows a decline of 5

mass transfer coefficient and incline of bulk concentration of the first membrane at 6

the 1st pass as a result to increasing the feed salinity. However, the case of the first 7

membrane located at the 2nd pass is quite comparable to the 1st pass due to the feeding 8

of low concentration stream. Specifically, the mass transfer coefficient of the 2nd pass 9

is noticeably higher than the mass transfer coefficient of the 1st pass due to lower bulk 10

concentration for all the membranes located at the 2nd pass. Koutsou et al. [32] 11

confirmed that the increase of bulk concentration in spiral wound modules causes an 12

increase of concentration polarisation, which associated with retarding mass transfer 13

coefficient. Therefore, it can be said that the mass transfer coefficient can 14

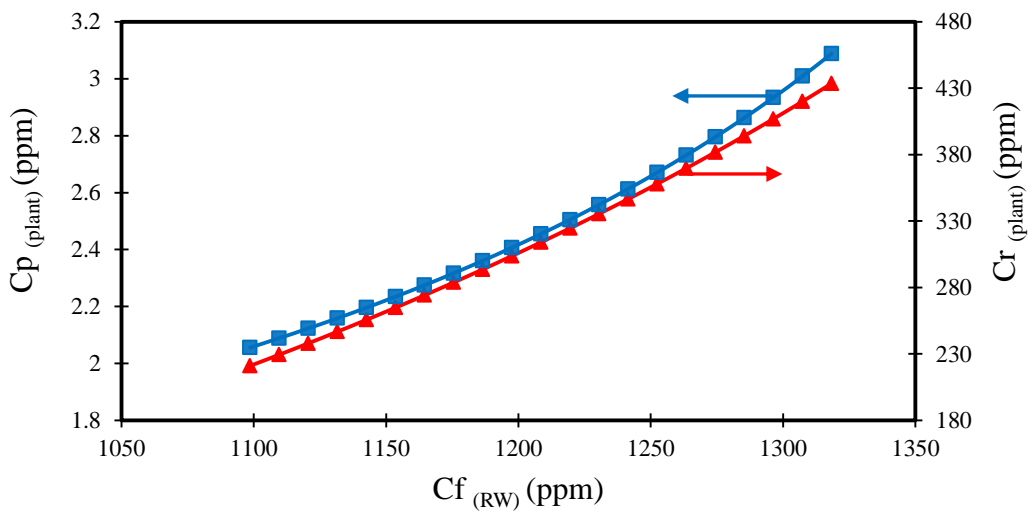significantly determine the concentration polarisation. 15

16

Fig. 2. Impact of feed water salinity on product and retentate salinity 18
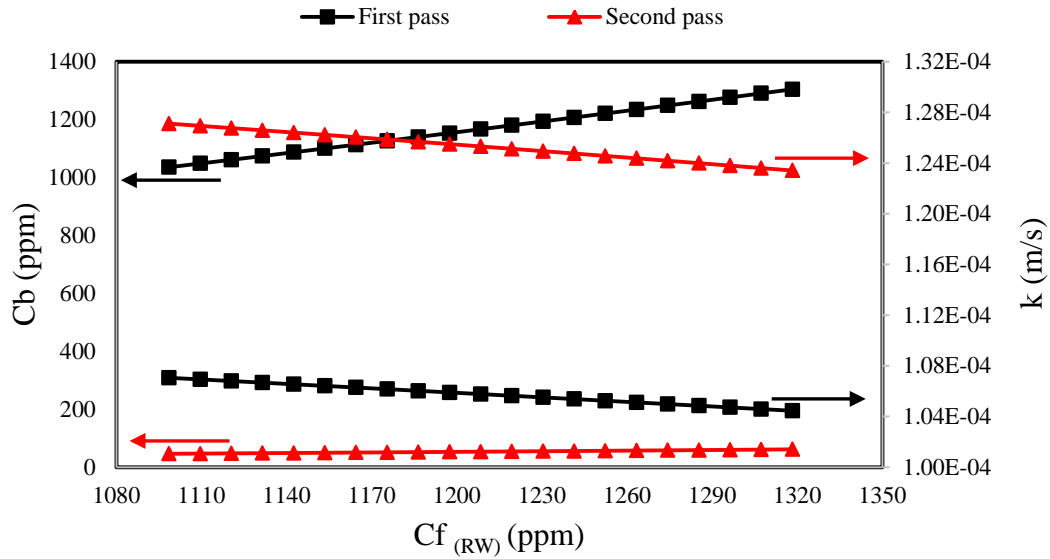
17

19

Fig. 3. Impact of raw water feed concertation on bulk concentration and mass transfer coefficient of the first membrane of passes 1 and 2

The total recoveries of plant, 1st pass, and 2nd pass are plotted against the variation of raw water concertation in Fig. 4. The total plant and 2nd pass recoveries are increased by 6% and 7% from 56.902% to 60.3924% and 81.75% to 87.64%, respectively. However, the 1st pass recovery is insignificantly impacted despite a trivial reduction. Increasing feed water salinity has increased the bulk concentration of each membrane and concertation polarisation in the 1st pass. This in turn reduces the water flux of each membrane and reduces the recovery of 1st pass. In contrast, the recovery of 2nd pass slightly increases as a response to increasing feed water salinity (Fig. 4) due to a continuous reduction of permeate recovery of 1st pass, which reduces the inlet feed flow rate of 2nd pass and enhances the recovery rate. Moreover, the characteristics of low feed salinity of 2nd pass serves the water flux. Consequently, the total plant recovery enhances as a response to increasing feed water salinity.
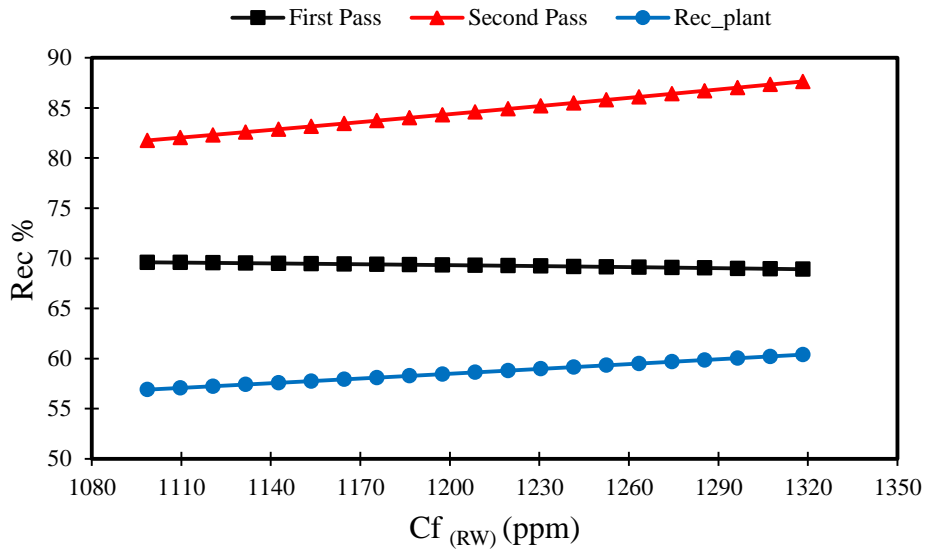
21

Fig. 4. Impact of raw water feed concertation on total recovery of passes 1 and 2

5.2 Impact of feed water flow rate

The impact of a 20% increase of feed water flow rate from 74 to 88.8 m³/h is studied against the plant performance at fixed feed water concentration 1098.62 ppm, operating pressure 9.22 atm and temperature 25 °C. In this case, changing the feed water flow rate causes a simultaneous change in both inlet plant feed flow rate and concentration, which are basically calculated based on mass and material balance equations. The model predictions of this case are plotted in Figs. (5) and (7) for total plant rejection, plant recovery, product concentration and plant retentate concentration, respectively.

It is observed that a 20% increase of feed water flowrate has insignificant impact on total plant solute rejection (99.798- 99.823%), 1st pass rejection (95.503- 96.051%) and 2nd pass rejection (95.521- 95.530%). Most importantly, an inconsiderable increase of plant solute rejection is occurred due to increasing feed water feed flow rate by 20%. However, it is also noticed that implementing a higher feed water flow rate is consistently led to a higher solute rejection compared to the case of 20%. A clear increase of boron rejection is occurred as a result to increasing the cross-flow velocity by 200% [33]. In fact, increasing cross-flow velocity leads to higher turbulence in the feed channel, which minimises the concentration polarisation and enhances mass transfer coefficient, permeate concentration and solute rejection. This fact is already pictured in Fig. 6, where the increase of feed water flowrate causes a noticeable increase of mass transfer coefficient in the feed-spacer channel of the first

22

membrane located at the 1st pass of the plant. This is already expected for all the membranes located at the 1st pass. Indeed, increasing the feed flowrate would be associated with increasing the Reynolds number (Fig. 6) due to increasing the bulk velocity. The latter are of course very important because flow features and mass transfer in spacer-filled channels, Reynolds number and Schmidt number (the physical parameters) are typically related [34]. It is emphasized that the simulation results in this study show that the Reynolds number values defined on the basis of superficial velocity in the first membranes of the 1st and 2nd passes did not exceed 200 (laminar flow) (Fig. 6), which is within the typical values reported for flow in spacer-filled channels [32]. However, the simulation Schmidt number is between $613 - 626$ that corresponding to the first membranes at the 2nd and 1st passes, respectively.

In this respect, increasing feed water flow rate causes a considerable reduction of total plant recovery (14.8%) and 1st pass recovery (14.7%) (Fig. 5). It is concluded that a maximum recovery is found at the lowest feed flow rate. This is attributed to increasing feed velocity at any compartment of RO vessels. This in turn means lower residence time of operation inside the module and lower water flux through the membrane. Also, increasing bulk velocity causes an increase in pressure losses along the feed channel that passively impacts the effective driving pressure despite the expected positive impact on reducing concentration polarisation. However, it is noticed that increasing feed water flow rate keeps a relatively fixed recovery of 2nd pass around 81.7% (Fig. 5). It must be noted that the calculation of total water recovery is based on the division of total product flowrate and the feed flowrate as given in Eq. (30). The progressive reduction of recovery rate of the 1st pass is because of the incomparable improvement of permeate flow rate against the increase of feed flow rate. Despite that the recovery of 1st pass decreases due to increasing feed water flow rate, the simulation results show a little positive increase of the permeate flow rate of the 1st pass, which in turn slightly increases the operating feed flow rate of 2nd pass. This in turn modifies the water flux in the 2nd pass due to keeping a fixed mass transfer coefficient (Fig. 6). Specifically, Fig. 6 shows no significant change of Reynolds number and mass transfer coefficient in the first membrane of the 2nd pass after increasing the water feed flowrate, which are nearly fixed at constant values. However, a deep looking at the simulation results shows a slight increase of the Reynold number and mass transfer coefficient in the first membrane of the 2nd pass (Fig. 6) and all the membranes located at the 2nd pass. This is due to a slight

improvement of feed flow rate of the 2nd pass that commensurate with a little increase of water flux at the first membrane of the 2nd pass after increasing the water feed flow rate. This in turn can explain the reason of a continuous reduction of both product and plant retentate concentrations due to decreasing operating feed flow rate of 2nd pass (Fig. 7). Statistically, the considered increase of feed water flowrate causes a reduction of 11% from 1.99 ppm to 1.768 ppm and 11% from 243.8 ppm to 208.4 ppm for product and plant retentate concentrations, respectively. Moreover, this analysis suggests that the total plant recovery should be lowered (Fig. 5) to ensure lower product concentration (Fig. 7). This is coordinate with the findings of Oh et al. [15].
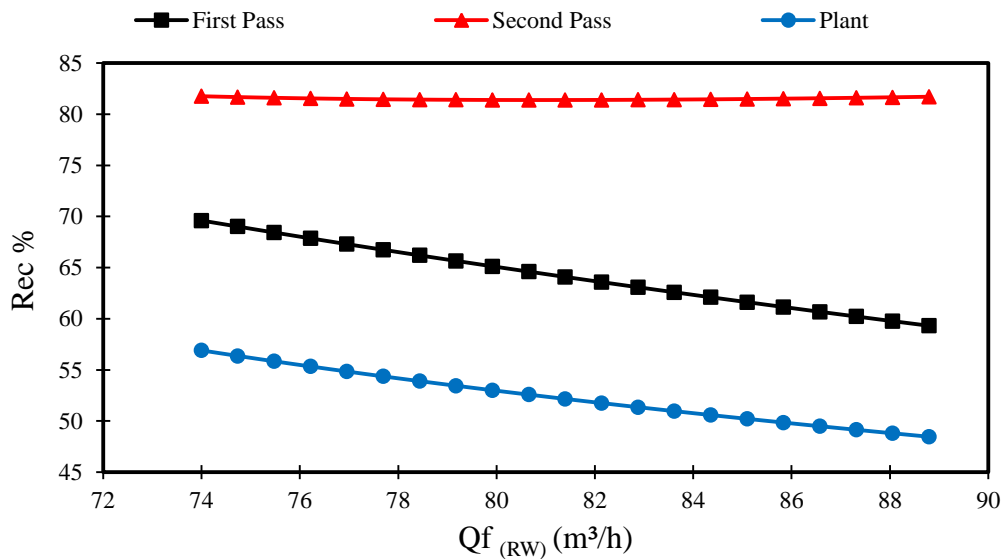

Fig. 5. Impact of feed water feed flowrate on total recovery of plant, passes 1 and 2
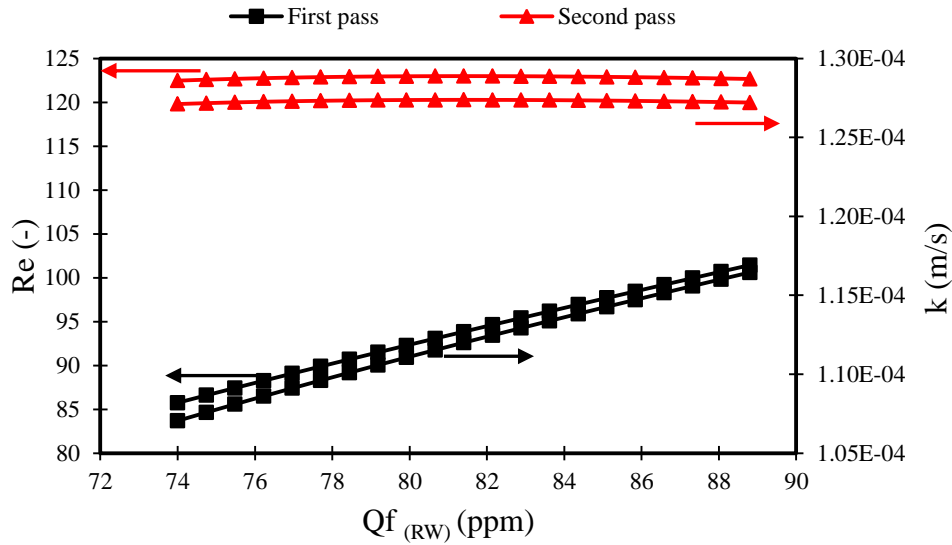
Fig. 6. Impact of feed water feed flowrate on Reynolds number and mass transfer coefficient of the first membrane of passes 1 and 2
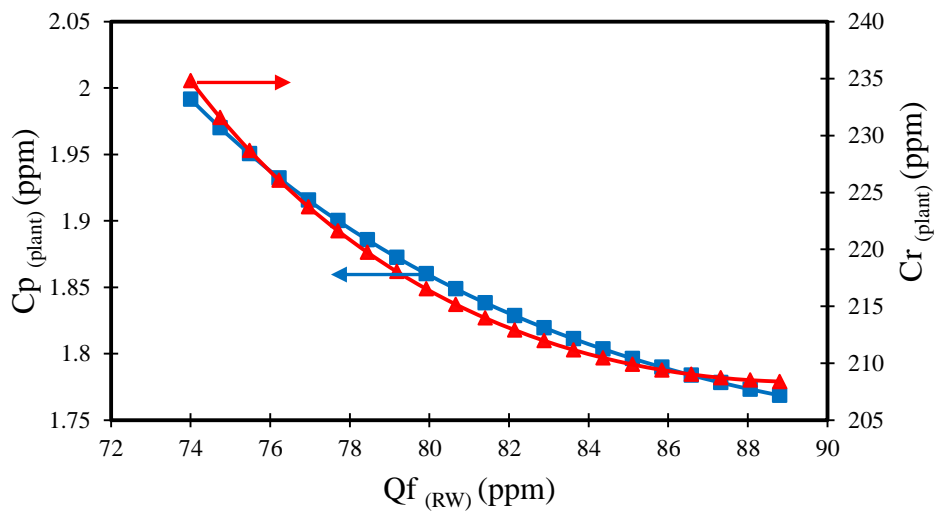

Fig. 7. Impact of feed water feed flowrate on product and retentate plant concentrations

5.3 Impact of inlet feed pressure

The range of 9.87 – 14.8 atm is the most membrane manufacturer's suggestion as the operating pressure of BWRO plants [33]. However, this study tested the impact of only 20% increase of operating feed pressure from 9.22 atm to 11.06 atm in the plant performance at fixed feed water concentration 1098.62 ppm, feed water flow rate 74 m³/h and temperature 25 °C.

As the operating pressure increases by 20%, no significant change is noticed in the total plant salt rejection (99.798 - 99.835%), 1st pass rejection (95.503 – 95.429%) and 2nd pass rejection (95.521 - 96.405%). The slight positive trend of plant solute rejection is attributed to higher water flux through the membranes, which leads to lowering the permeate concentration. Eq. (39) confirms that any improvement of recovery rate would positively serve the reduction of permeate concentration at the permeate channel. Also, increasing operating pressure aids to increasing mechanical compaction of membrane, which in turn decreases membrane pore size and increases membrane rejection [35].

Fig. 8 shows an exponential relationship for the product and plant retentate salinity against the increase of operating pressure. Therefore, Fig. 8 shows an optimal value of operating pressure, which relatively minimises the retentate salinity and commensurate with minimum product salinity. Fig. 8 shows that 10.6 – 10.88 atm is the optimal value of operating pressure that generates the lowest product concentration. Statistically, the product salinity is decreased by 22% from 1.99 ppm to 1.55 ppm besides the plant retentate salinity decreasing by 15% exponentially from 234.8 ppm to 198.6 ppm because of increasing operating pressure (Fig. 8). It is obvious that the retentate plant stream is relevant to the 2nd pass where the retentate stream of the 1st pass is disposed out the system (Fig. 1). In this respect, increasing the plant operating pressure would increase the total water permeation through the membranes of the 1st pass, which in turn increases the feed flow rate of high-quality water at the 2nd pass. Consequently, it is expected that any further increase of feed flow rate at the 2nd pass would reduce the permeate flow rate and recovery of this pass besides increasing the retentate flow rate and decreasing the retentate concentration. Occasionally, Eq. (40) indicates that any improvement of solute rejection in the 2nd pass will gain an advantage of reducing the retentate concentration.
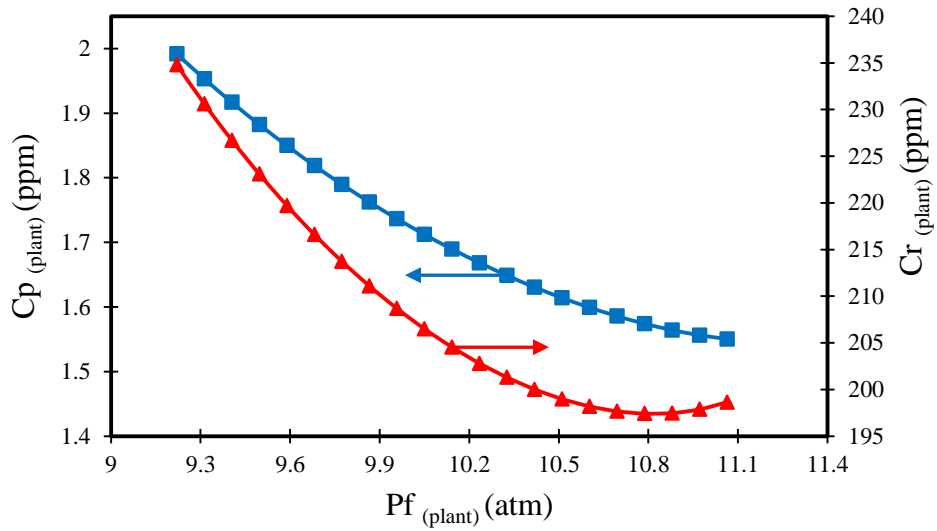
Fig. 8. Impact of plant operating pressure on product and retentate plant salinity

Fig. 9 shows a linear relationship between the total plant recovery, 1st pass recovery and 2nd pass recovery against the operating feed pressure. These results are in an agreement with Eq. (1) where any increase of pressure causes an increase of water flux. Accordingly, it is noticed that the operating pressure increase has a considerable positive impact of 13.4% on total plant recovery and 17.5% on 1st pass recovery compared to 3.5% reduction on 2nd pass recovery. This is explained as increasing recovery of 1st pass means higher feed flow rate of 2nd pass. This in turn reduces the positive impact of increasing operating pressure, which can attribute the insignificant decrease of recovery of 2nd pass. These results are coordinate with the findings of Jiang et al. [36].
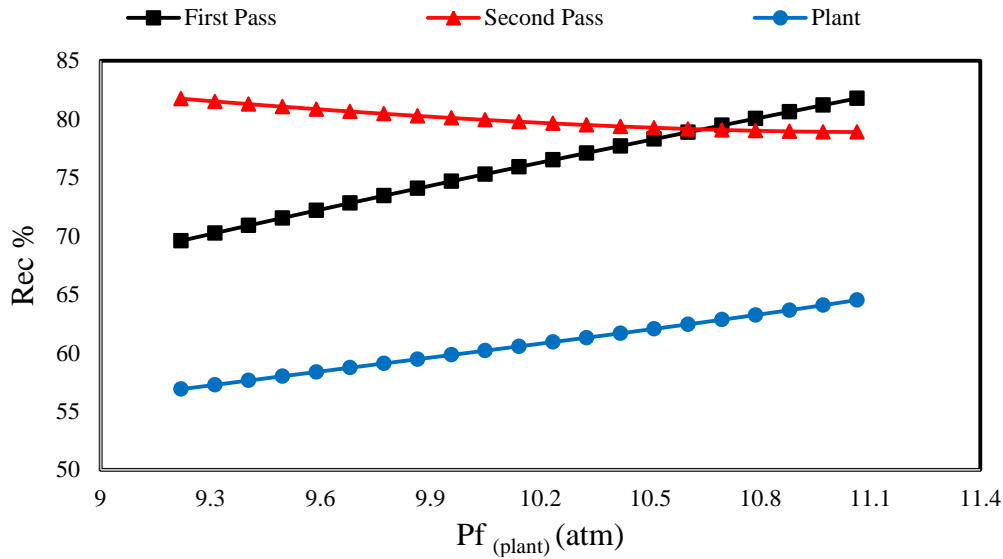
1
2
3
4
5
6
7
8
9
10
11
12
13
14

27

Fig. 9. Impact of plant operating pressure on total recovery of plant, passes 1 and 2

However, it is noticed that increasing operating pressure from 9.22 atm to 13 atm of 41% increase results in 11 ppm, 14619 ppm, 92.87%, 93.51%, and 99.31% of product concentration, plant retentate concentration, total plant recovery, 1st pass recovery and 2nd pass recovery, respectively. This shows a considerable advantage of total recovery compared to the first simulated results of a 20% increase to 11.06 atm of operating pressure. Therefore, it can be said running the process at 13 atm is a paramount key of process improvement due to generating low salinity level of product water.

5.4 Impact of inlet feed temperature

The variation of temperature in summer and winter seasons does not interfere much in the system, mainly because the feed water is pumped into large closed tanks, so the temperature inside the tank does not change much and mainly varies between 25 and 30 °C due to the season variation. Note that the feed water temperature has been quite constant at 25 °C at the time of data collection. Therefore, the simulation study is achieved to study the impact of temperature variation from 25 to 30 °C, which is already 20% variation, on the plant performance at fixed other operating parameters of feed water concentration 1098.62 ppm, feed water flow rate 74 m³/h and pressure 9.220 atm.

It is clearly observed that the increase of operating temperature has negligible impact on total plant solute rejection (99.798 - 99.641%), 1st pass rejection (95.503 - 93.61%), and 2nd pass rejection (95.521 - 94.387%). This is a slight reduction of plant

28

solute rejection which occurred as a result to increasing the solute transport permeability (Eq. 15). Specifically, increasing feed temperature affects both the membrane structure, transport parameters of water and solute in addition to physical properties. Consequently, increasing temperature results in increasing solute flux through each membrane, which causes a slight reduction of solute rejection due to increasing the permeate concentration at the permeate channel and following Eqs. (31) and (36). This is mostly reported by several researchers such as Mane et al. [37] and Kotb et al. [38].

Fig. 10 shows that increasing operating temperature would considerably increase the product salinity by 79% 1.99 ppm to 3.58 ppm accompanied by increasing retentate salinity by 50% from 234.8 ppm to 353.4 ppm.
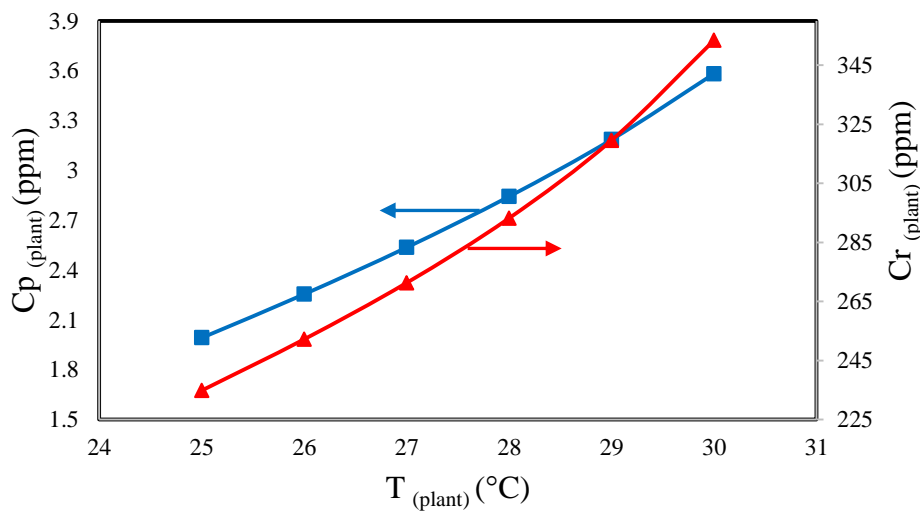

Fig. 10. Impact of plant operating temperature on product and retentate plant concentrations

In this respect, any increase of operating temperature would increase water transport parameter and decreases water viscosity. Therefore, it is expected that water recovery increases due to increasing water temperature. Fig. (11) shows an increase in total plant recovery (13%), 1st pass (11.6%) at a slight increase of 1.25% of 2nd pass recovery as a response to increasing temperature. Therefore, it can be said that the lower operating temperature serves the solute rejection at the penalty of lower recovery.
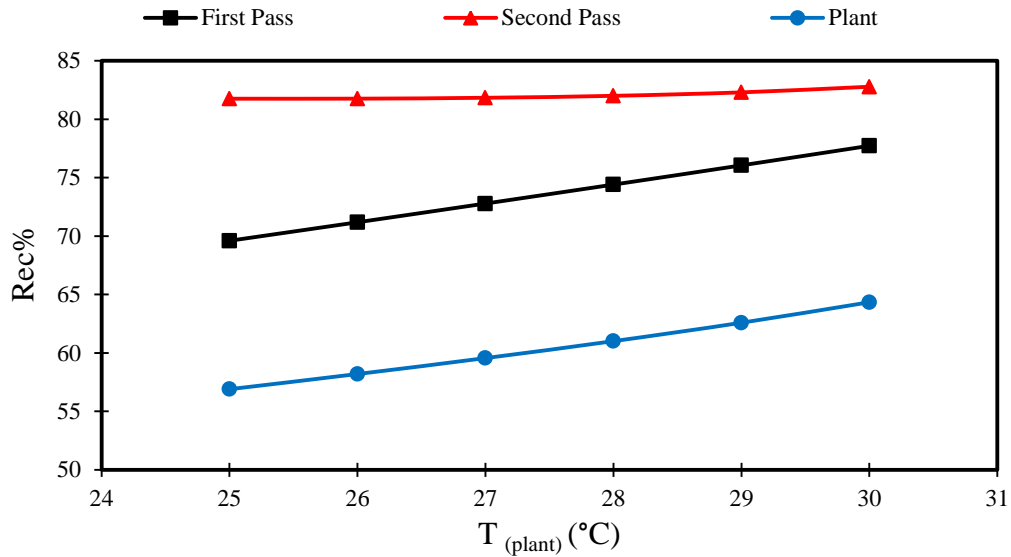
Fig. 11. Impact of plant operating temperature on total recovery of plant, passes 1 and 2

6. Conceptual suggestions to enhance the APC desalination plant performance

It is fair to mention that the recent multistage RO desalination plant design has met the severe requested low-salinity water (TDS lower than 2 ppm) considering both economic and environmental objectives. However, several suggestions are made to enhance the plant performance as follows:

- Energy recovery device is a component that reduces energy consumption and its implementation is quite important for BWRO desalination plant of APC. The forecasted reduction of energy consumption is would be more than half the energy consumed in the design of BWRO desalination plant without recovery device [39].
- Pumping the feed water at higher operating pressure is more economical and would enhance the plant recovery and product concentration especially when using energy recovery devices.
- The media-filter stage is recently used as a pre-treatment step. The implementation of nanofiltration would enhance the production of very low salinity water at reduced cost [40].

7. Conclusions

Mathematical model applicable for low-salinity Arab Potash Company (APC) brackish water medium-sized RO desalination plant located in Jordan is developed based on an explicit model developed for a spiral wound RO process. A number of

new expressions have been suggested for solute rejection and recovery rate besides the use of specific correlations to estimate the impact of operating temperature on model transport parameters. The model looks at the impact of operating conditions on the physical properties of the solution by considering of variable mass transfer coefficient and concentration polarization. The model prediction has been compared against actual operating data and deduced a good agreement of negligible errors and therefore used to analyse the impact of operating conditions in a sensitivity simulation study. The simulation is carried out at a specific range of operating conditions within 20% increase from the base case of actual plant data. The study assessed the impact of several operational parameters including feed salinity, feed water flow rate, operating pressure, and temperature in the BWRO plant performance. This in turn aids to understand the impact of operating parameters on the plant performance and elucidates the extent of the plant performance.

The sensitivity analysis of 20% variation of operating parameters shows ta number of observations:

- insignificant impact on total plant solute rejection for all the tested operating conditions. Specifically, the plant solute rejection is slightly reduced with feed water salinity and operating temperature. While, it is slightly increased with feed water flow rate and operating pressure;

- the total plant recovery is somewhat increased with feed water salinity, significantly decreased with feed water flow rate, significantly increased with operating pressure and temperature;

- feed water flow rate and operating pressure positively affect the product salinity while feed water salinity and operating temperature negatively affect.

The mathematical modelling of APC brackish water RO plant presented in this paper is a useful tool to investigate the plant performance for a long-time operation due to the expectation of performance decline due to fouling and scaling problems. Also, it will facilitate the plant optimisation studies required to identify the most effective methods of energy saving. Interestingly, the model developed can be used to estimate the performance of RO seawater desalination of any plant size.

Nomenclature

A_m : Effective area of the membrane (m²)

$A_{w(T)}$: Water transport coefficient at operating temperature (m/atm s)

A^* : The spacer characteristics (dimensionless)

$B_{s(T)}$: Solute transport coefficient at operating temperature (m/s)

C_b : The bulk solute concentrations at the feed channel (kg/m³)

C_f : The operating feed solute concentrations at the feed channel (kg/m³)

$C_{f(RW)}$: The feed water feed concentration (kg/m³)

C_w : The solute concentration on the membrane surface at the feed channel (kg/m³)

C_p : The permeate solute concentration at the permeate channel (kg/m³)

C_r : The retentate solute concentration of a membrane module (kg/m³)

C_{td} : The total drag coefficient (dimensionless)

D_b : The solute diffusion coefficient of feed at the feed channel (m²/s)

d_h : The hydraulic diameter (m)

Q_s : The solute flux through the membrane (kg/m² s)

J_w : The water flux through the membrane (m/s)

k : The mass transfer coefficient at the feed channel (m/s)

k_{dc} : Constant in Eq. (19) (dimensionless)

L : The membrane length (m)

m_f : Parameter in Eq. (22)

n : The spacer characteristics (dimensionless)

P_f : The operating feed pressure of a membrane module (atm)

P_r : The retentate pressure of a membrane module (atm)

P_p : The permeate channel pressure of a membrane module (atm)

Q_b : The bulk feed flow rate at the feed channel of a membrane module (m³/s)

Q_f : The operating feed flow rate at the feed channel of a membrane module (m³/s)

$Q_{f(RW)}$: The feed water feed flow rate (m³/s)

Q_p : The permeate flow rate at the permeate channel of a membrane module (m³/s)

Q_r : The retentate flow rate at the feed channel of a membrane module (m³/s)

Re_b : The Reynolds number of the bulk at the feed channel (dimensionless)

Rec : Total permeate recovery of a membrane module (dimensionless)

Rej : The observed solute rejection of a membrane module (dimensionless)

Rel_{ac} : The accurate solute rejection of a membrane module (dimensionless)

T : The operating feed temperature of a membrane module (°C)

t_f : Height of feed channel (m)

U_b : The bulk feed velocity at the feed channel of a membrane module (m/s)

W : The membrane width (m)

Subscript

μ_b : The bulk viscosity at the feed channel of a membrane module (kg/m s)

ρ_b : The bulk density at the feed channel of a membrane module (kg/m³)

$\Delta P_{drop,E}$: The pressure drop of the spiral wound element (atm)

π_b : The bulk osmotic pressure at the feed channel (atm)

π_p : The osmotic pressure at the permeate channel (atm)

ϵ : The void fraction of the spacer (dimensionless)

References

[1] T. Qasim, M.S. Obeidat, H. Smadi, Technical and Technical and Technical and Technical and Economical Evaluation of a of a of a Fresh-Water Production from Zero-Wastewater Reverse Osmosis Syste: A FeasibilityStudy in Jordanin, Review of European Studies 10(2) (2018) 53–59.

[2] G.E. Ahmad, J. Schmid, Feasibility study of brackish water desalination in the Egyptian deserts and rural regions using PV systems, Energy Conversion and Management 43 (2002) 2641–2649.

[3] M.A. Alghoul, P. Poovanaesvaran, K. Sopian, M.Y. Sulaiman, Review of brackish water reverse osmosis (BWRO) system designs, Renewable and Sustainable Energy Reviews 13 (2009) 2661–2667.

[4] A. Altaee, N. Hilal, High recovery rate NF–FO–RO hybrid system for inland brackish water treatment, Desalination 363 (2015) 19–25.

[5] M.S. Mousa, O.R. A1-Jayyousi, Brackish water desalination: an alternative for water supply enhancement in Jordan, Desalination 124 (1999) 163–174.

[6] L. Zhao, P.C.-Y. Chang, W.S.W. Ho, High-flux reverse osmosis membranes incorporated with hydrophilic additives for brackish water desalination, Desalination 308 (2013) 225–232.

[7] P. Xu, M. Capito, T.Y. Cath, Selective removal of arsenic and monovalent ions from brackish water reverse osmosis concentrate, Journal of Hazardous Materials 260 (2013) 885–891.

[8] K.M. Sassi, I.M. Mujtaba, Effective design of reverse osmosis based desalination process considering wide range of salinity and seawater temperature, Desalination 306 (2012) 8–16.

[9] K.M. Sassi, I.M. Mujtaba, Optimal operation of RO system with daily variation of freshwater demand and seawater temperature, Computers and Chemical Engineering 59 (2013) 101–110.

[10] C.-J. Lee, Y.-S. Chen, G.-B. Wang, A dynamic simulation model of reverse osmosis desalination systems. The 5 th International Symposium on Design, Operation and Control of Chemical Processes, PSE Asia, Singapore, 2010.

[11] A. Abbas, N. Al-Bastaki, Performance decline in brackish water Film Tec spiral wound RO membranes, Desalination 136(1) (2001) 281–286.

[12] S. Bouguecha, B. Hamrouni, M. Dhahbi, Operating analysis of a direct energy coupled desalination family prototype, Desalination 168 (2004) 95–100.

[13] S. Senthilmurugan, A. Ahluwalia , S.K. Gupta, Modeling of a spiral-wound module and estimation of model parameters using numerical techniques, Desalination 173 (2005) 269–286.

[14] A. Abbas, Simulation and analysis of an industrial water desalination plant, Chemical Engineering and Processing: Process Intensification 44(9) (2005) 999–1004.

[15] H.-J. Oh, T.-M. Hwang, S. Lee, A simplified simulation model of RO systems for seawater desalination, Desalination 238 (2009) 128–139.

[16] T. Kaghazchi, M. Mehri, M.T. Ravanchi, A. Kargari, A mathematical modeling of two industrial seawater desalination plants in the Persian Gulf region, Desalination 252 (2010) 135–142.

34

[17] M.A. Al-Obaidi, C. Kara-Zaitri, I.M. Mujtaba, Scope and limitations of the irreversible thermodynamics and thesolution diffusion models for the separation of binary andmulti-component systems in reverse osmosis process, Computers and Chemical Engineering 100 (2017) 48–79.

[18] V. Geraldes, N.E. Pereira, M.N. de Pinho, Simulation and optimization of medium-sized seawater reverse osmosis processes with spiral-wound modules, Ind. Eng. Chem. Res. 44 (2005) 1897–1905.

[19] F. Majali, H. Ettouney, N. Abdel-Jabbar, H. Qiblawey, Design and operating characteristics of pilot scale reverse osmosis plants, Desalination 222 (2008) 441–450.

[20] J. Marriott, E. Sørensen, A general approach to modelling membrane modules, Chemical Engineering Science 58 (2003) 4975-4990.

[21] S. Lee, R.M. Lueptow, Rotating reverse osmosis: a dynamic model for flux and rejection, Journal of Membrane Science 192 (2001)129-143.

[22] E. Ruiz-Saavedra, A. Ruiz-García, A. Ramos-Martín, A design method of the RO system in reverse osmosis brackish water desalination plants (calculations and simulations), Desalination and Water Treatment (2014) 1–11. doi: 10.1080/19443994.2014.939489.

[23] R. Bashitialshaaer, K.M. Persson, M. Aljaradin, The Dead Sea Future Elevation, Int. J. of Sustainable Water and Environmental Systems 2 (2011) 67–76.

[24] Arab Potash Company, PLC, 2011. Annual report, www.arabpotash.com (Accessed on 10/3/2018).

[25] H.K. Lonsdale, U. Merten, R.L. Riley, Transport properties of cellulose acetate osmotic membranes, Journal of Applied Polymer Science 9 (1965)1341–1362.

[26] A.R. Da Costa, A.G. Fane, D.E. Wiley, Spacer characterization and pressure drop modelling in spacer-filled channels for ultrafiltration, J. Membr. Sci. 87 (1994) 79–98.

[27] Toray Membrane USA Inc., membrane technology solutions. Operation, Maintenance and Handling Manual, 2015. http://www.toraywater.com/ (Accessed on 10/3/2018).

[28] A.S. Michaels, New separation technique for the chemical process industries, Chem. Eng. Prog. 64 (1968) 31-34.

[29] C. Koroneos, A. Dompros, G. Roumbas, Renewable energy driven desalination systems modelling, J. Clean. Prod. 15 (2007) 449-464.

[30] R.W. Lawrence, Calculation of the expected performance of reverse osmosis plants, Desalination 42 (1982) 247–253.

[31] K.M. Sassi, I.M. Mujtaba, Optimal design and operation of reverse osmosis desalination process with membrane fouling, Chemical Engineering Journal 171 (2011) 582– 593.

[32] C.P. Koutsou, S.G. Yiantsios, A.J. Karabelas, A numerical and experimental study of mass transfer in spacer-filled channels: Effects of spacer geometrical characteristics and Schmidt number, Journal of Membrane Science 326 (2009) 234– 251.

[33] A. Farhat, F. Ahmad, N. Hilal, H.A. Arafat, Boron removal in new generation reverse osmosis (RO) membranes using two-pass RO without pH adjustment, Desalination 310 (2013) 50–59.

[34] A.R. Da Costa, A.G. Fane, C.J.D. Fell, A.C.M. Franken, Optimal channel spacer design for ultrafiltration, J. Membrane Sci. 62 (1991) 275–291.

[35] D.M. Bohonak, A.L. Zydney, Compaction and permeability effects with virus filtration membranes, Journal of Membrane Science 254 (2005) 71–79.

[36] A. Jiang, Q. Ding, J. Wang, S. Jiangzhou, W. Cheng, C. Xing, Mathematical Modeling and Simulation of SWRO Process Based on Simultaneous Method, Journal of Applied Mathematics (2014) 1–11. http://dx.doi.org/10.1155/2014/908569.

[37] P.P. Mane, P.-K. Park, H. Hyung, J.C. Brown, J.-H. Kim, Modeling boron rejection in pilot- and full-scale reverse osmosis desalination processes, Journal of Membrane Science 338 (2009) 119–127.

[38] H. Kotb, E.H. Amer, K.A. Ibrahim, Effect of operating conditions on salt concentration at the wall of RO membrane, Desalination 357 (2015) 246–258.

[39] A. Villafafila, I.M. Mujtaba, Fresh water by reverse osmosis based desalination: simulation and optimisation, Desalination 155 (2003) l–13.

[40] N. Hilal, A.W. Mohammad, B. Atkin, N.A. Darwish, Using atomic force microscopy towards improvement in nanofiltration membranes properties for desalination pre-treatment: a review, Desalination 157 (2003) 137–144.

1

2

3

4

5

6

7

Appendix A

Table A.1. The mathematical modelling of APC brackish water RO desalination plant

Model Equations	Specifications	Eq. no
$Q_{f(plant)} = RR\ Q_{r(plant)} + Q_{f(RW)}$	Plant feed flow rate (RR is the retentate ratio)	1
$Q_{f(plant)}\ C_{f(plant)} = RR\ Q_{r(plant)}\ C_{r(plant)} + Q_{f(RW)}\ C_{f(RW)}$	Plant feed concentration	2
$Q_{r(plant)} = Q_{r(pass=2)}$	Plant retentate flow rate	4
$C_{r(plant)} = C_{r(pass=2)}$	Plant retentate concentration	5
$C_{p(Plant)} = C_{p(pass=2)}$	Plant product concentration	7
$Q_{p(Plant)} = Q_{p(pass=2)}$	Plant permeate flow rate	6
$T_{f(plant)} = T_{r(plant)}$	Plant constant temperature	10
$P_{r(plant)} = P_{r(pass=2)}$	Plant retentate pressure	9
$Rec_{(plant)} = \dfrac{Q_{p(plant)}}{Q_{f(plant)}}\ x100$	Total plant permeate recovery	15
$Rej_{(plant)} = \dfrac{C_{f(plant)} - C_{p(plant)}}{C_{f(plant)}}\ x100$	Total plant rejection	14
$C_{f(pass=1)} = C_{f(plant)}$	Feed concentration of 1st pass	11
$Q_{f(pass=1)} = Q_{f(plant)}$	Feed flow rate of 1st pass	3
$Q_{p(pass=1)} = \displaystyle\sum_{PV=1}^{10} Q_{p(PV)}$	Permeate flow rate of 1st pass	12
$C_{p(pass=1)} = \dfrac{\sum_{PV=1}^{10} C_{p(PV)}\ Q_{p(PV)}}{Q_{p(pass=1)}}$	Permeate concentration of 1st pass	
$Rej_{(pass=1)} = \dfrac{C_{f(pass=1)} - C_{p(pass=1)}}{C_{f(pass=1)}}\ x100$	Total 1st pass rejection	14
$Rec_{(pass=1)} = \dfrac{Q_{p(pass=1)}}{Q_{f(pass=1)}}\ x100$	Total 1st pass permeate recovery	15
$P_{f(pass=2)} = 1.066x\ P_{f(pass=1)}$	Feed pressure of 2st pass	8
$C_{f(pass=2)} = C_{p(pass=1)}$	Feed concentration of 2st pass	11
$Q_{p(pass=2)} = \displaystyle\sum_{PV=1}^{8} Q_{p(PV)}$	Permeate flow rate of 2st pass	13
$C_{p(pass=2)} = \dfrac{\sum_{PV=1}^{10} C_{p(PV)}\ Q_{p(PV)}}{Q_{p(pass=2)}}$	Permeate concentration of 2st pass	
$Rej_{(pass=2)} = \dfrac{C_{f(pass=2)} - C_{p(pass=2)}}{C_{f(pass=2)}}\ x100$	Total 2st pass rejection	14
$Rec_{(pass=1)} = \dfrac{Q_{p(pass=2)}}{Q_{f(pass=2)}}\ x100$	Total 2st pass permeate recovery	15